Synthesis, Structures and Photoluminescence Properties of a Series of Alkaline Earth Metal-Based Coordination Networks Synthesized Using Thiophene-Based Linkers

ARTICLE *in* CRYSTAL GROWTH & DESIGN · JANUARY 2013

Impact Factor: 4.89 · DOI: 10.1021/cg301471r

4 AUTHORS, INCLUDING:

Xianyin Chen
Stony Brook University
6 PUBLICATIONS **19** CITATIONS
SEE PROFILE

Anna M Plonka
Yeshiva University
18 PUBLICATIONS **113** CITATIONS
SEE PROFILE

Debasis Banerjee
Pacific Northwest National Laboratory
36 PUBLICATIONS **477** CITATIONS
SEE PROFILE

CRYSTAL GROWTH & DESIGN

Article

pubs.acs.org/crystal

Synthesis, Structures and Photoluminescence Properties of a Series of Alkaline Earth Metal-Based Coordination Networks Synthesized Using Thiophene-Based Linkers

Xianyin Chen,[†] Anna M. Plonka,[‡] Debasis Banerjee,*[,†] and John B. Parise*[,†,‡]

[†]Department of Chemistry, Stony Brook University, Stony Brook, New York, 11794-3400, United States

[‡]Department of Geosciences, Stony Brook University, Stony Brook, New York, 11794-2100, United States

Supporting Information

ABSTRACT: Three new 3-D coordination networks were synthesized using alkaline-earth metal centers, calcium, and strontium, with 2,5-thiophenedicarboxylate (TDC) as the organic linker. $[Ca_2(TDC\text{-}2H)_2(DMF)_2]_n$ [**1**, space group $P2_1/n$, a = 10.0704(3) Å, b = 14.2521(3) Å, c = 17.5644(6) Å, β = 94.281(2)°] is composed of tetrameric calcium polyhedral clusters, which are connected by the organic linkers. Coordinated DMF molecules are present within the 1-D channel along the [010] direction. $[Ca(TDC\text{-}2H)]_n$ [**2**, space group $Pbcm$, a = 5.3331(5) Å, b = 6.8981(4) Å, c = 18.141(2) Å] consists of chains of edge-sharing calcium octahedra, connected by organic linkers, to form a dense network. $[Sr(TDC\text{-}2H)(DMF)]_n$ [**3**, space group $P2_1/n$, a = 5.9795(3) Å, b = 17.058(1) Å, c = 11.3592(6) Å, β = 91.257(1)°] forms a structural topology almost identical to compound **1** except that the chains are built by combinations of edge- and face-sharing polyhedra. Compounds **1** and **3** were synthesized using DMF as solvent, whereas compound **2** crystallizes using ethanol. Photoluminescence studies reveal that the topologies of the networks and the presence of the coordinated solvent molecules control the luminescence properties of the compounds.

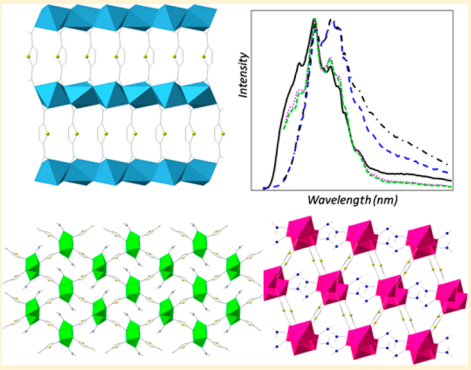

1. INTRODUCTION

metal−organic frameworks (MOFs) or coordination networks are crystalline solids comprising metal ions or a metal cluster, connected by multifunctional organic ligands, forming 1-D chains, 2-D layers, or 3-D networks.[1,2] A wide range of metal centers and functionalized organic linkers are used to form these materials, designed for specific application, such as gas-storage,[3−6] separation,[7−11] and sensing.[12,13] The structural topologies and properties of the synthesized materials can be tuned by altering synthetic parameters, such as the solvent[14−16] and temperature,[17] in addition to the metal centers and organic linkers.[18] First-row transition metal centers are popular choices to construct such networks because of their tendency to form robust secondary building units (SBUs)[19,20] and because of their well-known bonding interaction with the ligand functional groups.[21] On the other hand, *s*-block metal-based networks are relatively less studied. The use of early members of earth abundant *s*-block metal centers (Li, Mg, Ca) to construct porous networks can offer several advantages, ranging from networks with enhanced thermal stability to those of lower atomic weight, compared with MOFs containing transition metals.[22]

Apart from metal centers, the choice of organic linkers is crucial for building new *s*-block metal-based networks, as the mutual angle of the ligand functionalities determines network topologies.[23] Polycarboxylate linkers are widely popular, and the use of heterocyclic aromatic polycarboxylates as building blocks offers variable binding modes[24] to the metal centers, allowing access to novel network architectures and properties.[22,25] For example, 2,5-thiophenedicarboxic acid (TDC) is an ideal aromatic linker choice to build novel networks because of the diverse coordination modes of the carboxylate groups and the rigidity of the heterocyclic ring.[26,27] Reported different TDC coordination modes of Co-,[28] Cd-,[29] In-,[29] Ln- (Dy, Ho, Er),[30] Li-,[31] and Mg[32]-based networks include multidentate modes. In this study, the bridging, chelating or combination of both binding modes of $-COO^-$ moieties of TDC ligand are discussed. In addition, TDC is a photoluminescent molecule due to the delocalization of a sulfur lone pair within the heterocyclic ring,[33,34] which raises the possibility of obtaining a coordination network with luminescent properties that might vary with the nature of the gas or solvent molecule absorbed.

We are currently exploring the chemistry of *s*-block metal-based networks using different organic linkers and synthetic conditions with the aim of discovering novel lightweight sensing materials. In this work, we report the solvothermal synthesis, structural characterization, and luminescence properties of a series of *s*-block coordination networks using TDC as

Received: October 8, 2012
Revised: November 12, 2012
Published: November 21, 2012

Table 1. Crystallographic Data and Structural Refinement Details of Structures 1−3

compound	1	2	3
formula	$C_{18}H_{18}Ca_2N_2O_{10}S_2$	$C_6H_2CaO_4S$	$C_9H_{8.25}NO_5SSr$
formula weight	566.62	210.22	330.10
crystal system	monoclinic	orthorhombic	monoclinic
wavelength(Å)	0.71073	0.71073	0.41328
space group	$P2_1/n$	$Pbcm$	$P2_1/n$
a (Å)	10.0704(3)	5.3331(5)	5.9795(3)
b (Å)	14.2521(3)	6.8981(4)	17.058(1)
c (Å)	17.5644(6)	18.141(2)	11.3592(6)
α (°)	90.00	90.00	90.00
β (°)	94.281(2)	90.00	91.257(1)
γ (°)	90.00	90.00	90.00
volume (Å^3)	2513.9(1)	667.38(9)	1158.4(1)
Z	4	4	4
density$_{cacl}$(g/cm^3)	1.4971	2.092	1.893
μ (mm^{-1})	0.672	1.212	1.158
reflections, measured	44560	3093	22934
reflections, unique	5127	701	3455
reflections, observed [$I > 2\sigma(I)$]	4415	599	3149
R_{int}	0.0422	0.0333	0.0333
goodness of fit	1.070	1.063	1.244
R_1 [$I > 2\sigma(I)$]	0.0494	0.0289	0.0183
wR_2 [all data]	0.1519	0.0768	0.0715

the linker. Our study suggests that the network topology and the presence of the coordinated solvent molecules are important factors controlling the luminescence properties of the synthesized materials.

2. EXPERIMENTAL SECTION

2.1. Synthesis. Compounds **1**−**3** were synthesized under solvothermal conditions using Telfon-lined 23-mL Parr stainless steel autoclaves. Starting materials, include calcium nitrate tetrahydrate ($Ca(NO_3)_2{\cdot}4H_2O$, Acros-Organics, 99+% purity), strontium nitrate ($Sr(NO_3)_2$, Alfa-Aesar, 99.9%), 2,5-thiophenedicarboxylic acid ($C_6H_4O_4S$, TDC, Sigma-Aldrich, 95% purity), *N*,*N*′-dimethylformamide (C_3H_7NO, Sigma-Aldrich, 99% purity), and ethanol (Fisher, 95% purity), were used as received without further purification.

2.2. Synthesis of 1 $[Ca_2(TDC\text{-}2H)_2(DMF)_2]_n$. A typical synthesis includes a mixture of $Ca(NO_3)_2{\cdot}4H_2O$ [0.243 g, 1.03 mmol] and TDC [0.182 g, 1.06 mmol] dissolved in 10.24 g of DMF and stirred for 2 h to achieve homogeneity [molar ratio of metal salt/ligand/solvent = 1:1:140]. The resultant solution was heated for 5 days at 100 °C, and the product was collected by filtration as yellowish prismatic crystals, which were washed using DMF and allowed to air-dry. The yield was 74% based on Ca, 0.217 g.

2.3. Synthesis of 2 $[Ca(TDC\text{-}2H)]_n$. Compound **2** was synthesized from a mixture of $Ca(NO_3)_2{\cdot}4H_2O$ [0.239 g, 1.01 mmol] and TDC [0.179 g, 1.04 mmol] dissolved in 6.4 g of ethanol, which was stirred for 3 h [molar ratio of metal salt/ligand/solvent = 1:1:140]. The resultant solution was heated for 5 days at 100 °C. The product was collected by filtration as pale yellow plate-like crystals, which were rinsed with ethanol and allowed to air-dry. The yield was 97% based on Ca, 0.207 g.

2.4. Synthesis of 3 $[Sr(TDC\text{-}2H)(DMF)]_n$. Compound **3** was synthesized by dissolving $Sr(NO_3)_2$ [0.236 g, 1.12 mmol] and TDC [0.176 g, 1.02 mmol] in 10 g of DMF and stirring for 2 h [molar ratio of metal salt/ligand/solvent = 1:1:130]. The resulting solution was heated for 5 days at 100 °C. The product was obtained by filtration as yellowish prismatic crystals, which were washed with DMF and allowed to air-dry. The yield was 63.6% based on Sr, 0.234 g.

2.5. X-ray Crystallography. Representative crystals of compounds **1**−**3** suitable for single crystal X-ray diffraction were selected from the bulk samples and were mounted on glass fibers using epoxy adhesive. Data for compounds **1** and **2** were collected with 1° ω scans at 293 K using a four-circle kappa Oxford Gemini diffractometer equipped with an Atlas detector (λ = 0.71073 Å). The raw intensity data were collected, integrated, and corrected for adsorption effects using CrysAlis PRO software.[35] Reflections for compound **3** were collected at 100 K using a three-circle Bruker D8 diffractometer equipped with an APEXII detector (λ = 0.41328 Å) using 0.5° φ scans at Advanced Photon Source ChemMatCars beamline. The raw intensity data were collected, integrated and corrected for absorption effect with the Apex II software suite. The crystal structures of compounds **1**−**3** were solved using a direct method (SHELXS).[36] Metal and sulfur atoms were located first, followed by determination of other atom positions (C, O) from Fourier difference maps. Most of the non-hydrogen atoms were refined anisotropically (Supporting Information Figures S5−7). Hydrogen atoms were added to the structure model using geometrical constraints. A summary of some important crystallographic details can be found in Table 1. Powder X-ray diffraction (PXRD) data were collected to confirm phase purity using a Rigaku Ultima-IV diffractometer Cu Kα (λ = 1.5418 Å) with a range of $5 \leq 2\Theta \leq 40°$ (scanning rate: 1°/min). The powder patterns so collected were consistent with those simulated based on structure models derived from single crystal data (Supporting Information Figures S8−S10).

2.6. Thermal Analysis. Combined TGA-DSC data of **1**−**3** were collected using a STA 449 C Jupiter Netzsch Instrument. Powder samples were placed in an Al_2O_3 crucible and heated from 25 to 700 °C at a heating rate of 10 °C min^{-1} under N_2 atmosphere.

2.7. Photoluminescence. In preparation for fluorescence measurements, compounds **1**−**3** and the free TDC linker were ground into powder. Quartz slides of dimension 16 mm × 60 mm were first rinsed with deionized water and ethanol and dried, then black tape was applied to the lower half of the dried slide. The tape was then removed to leave behind a small amount of adhesive, onto which a continuous thin layer of sample was sprinkled. Excess sample was removed by gently tapping the slide face down. The effects of the glass slide and adhesive on the fluorescence were evaluated and found to be negligible. The excitation and emission spectra of thin layers of free TDC and solid samples of compounds **1**−**3** were measured on a Varian Cary Eclipse fluorescence spectrophotometer. The emission spectra were recorded with the excitation fixed at 300 nm, the excitation maximum of free TDC.

dx.doi.org/10.1021/cg301471r | Cryst. Growth Des. 2013, 13, 326−332

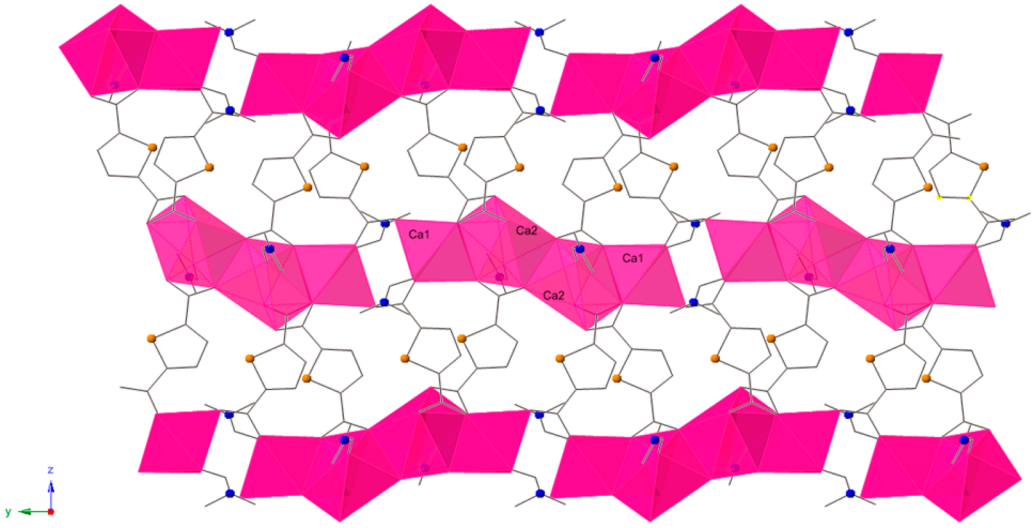

Figure 1. View of compound **1** along [100] showing the connectivity of the organic linkers with calcium metal centers. Calcium coordination polyhedra are pink, sulfur is showed in orange spheres, nitrogen in blue, and the carbons are represented by wire bonds. Hydrogen atoms were omitted for clarity.

3. RESULTS AND DISCUSSION

3.1. Structure of 1 [Ca(TDC-2H)(DMF)]$_n$. The asymmetric unit of **1** comprises two crystallographic unique calcium centers and two complete organic linkers with two coordinated DMF molecules. The two Ca centers located at two general positions lead to the Ca(1)Ca(2)Ca(2)Ca(1) tetramers. (Figure 1) The Ca(1) metal center (Supporting Information Figure S1) is coordinated to five carboxylate oxygen atoms of five different TDC-2H linkers and one oxygen atom from a solvent molecule, generating square bipyramidal geometry. The Ca(2) (Supporting Information Figure S2) is present in a pentagonal bipyramidal environment with seven oxygen atoms, from four TDC-2H linkers and one DMF molecule. The carboxylate groups of the TDC-2H ligands in **1** present type a, b, and c coordination modes (Scheme 1, Figure 2). The square bipyramidal geometry contains types of three a, one b3, and one c1 TDC-2H oxygen donors, whereas one type a, one b1, two b2, and two c2 binding modes are present in the pentagonal bipyramidal environment. The bond distances of Ca−O range from 2.256(3) Å to 2.504(2) Å, with an average of 2.356(2) Å (Table 2). O(6) and O(7) are coordinated to both Ca(1) and Ca(2), and the Ca(1)−O(6) and Ca(2)−O(6) bond lengths are lengthened to 2.431(2) Å and 2.504(2) Å, respectively. Similarly, a longer Ca(2)−O(7) bond distance of 2.484(2) Å is observed. The average Ca−O bond length of binding modes a in **1** is 2.292(3) Å; b1, 2.360(3) Å; b2, 2.388(2) Å; b3, 2.343(2) Å; c1, 2.431(2) Å; and c2, 2.472(2) Å. As expected, Ca−O bond distances increase from monodentate to multidentate modes. DMF molecules coordinating to the calcium metal centers run along the channels of the crystallographic [010] direction. The two Ca^{2+} sites in different coordination modes forming an edge-sharing tetrameric unit, connecting with another eight tetramers via TDC-2H ligands, result in the 3-D frameworks.

Scheme 1. Coordination Modes of the −COO$^-$ Moieties of TDC Linker (a) Bridging, (b) Chelating and Bridging with One Oxygen, (c) Chelating and Bridging with Two Oxygens, and (d) Bridging with Two Metals and Bridging with One Metal

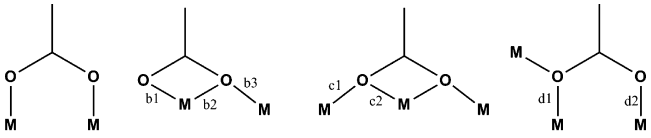

3.2. Structure of 2 [Ca(TDC-2H)]$_n$. The asymmetric unit of **2** includes a unique calcium ion, localized on the 2-fold rotation axis and a half of the TDC-2H linker, with the sulfur atom localized on the mirror plane. The Ca is coordinated to six oxygen atoms from six independent linkers (Supporting Information Figure S3), forming the 1-D octahedral chains. In the overall structure, the TDC linker is associated with six calcium ions, as carboxylate oxygen O1 coordinates to one calcium ion and carboxylate oxygen O2 coordinates to two metal centers. The calcium on the rotation axis shows a distorted octahedral geometry containing four d1 and two d2 types of carboxylate oxygen donors. (Figure 2) Comparing the average Ca−O bond lengths—the 2.300(2) Å bond distance of binding mode d2 observed in **2** to the average 2.3935(10) Å of type d1 (Table 3)—the Ca−O bond distances increase from the bridging mode to the chelating mode. The structure of **2** can be described as a 3-D dense coordination network formed by one-dimensional edge-sharing chains of calcium octahedra, which are linked by a TDC-2H ligand (Figure 3).

3.3. Structure of 3 [Sr(TDC-2H)(DMF)]$_n$. The asymmetric unit of **3** comprises one crystallographically unique strontium atom, one independent linker, and one DMF molecule. The Sr metal center is found in an 8-fold coordination environment with seven of its oxygens coming from six TDC-2H linkers, and one contributed by a coordinated DMF molecule (Supporting Information Figure S4). The coordinated DMF molecule running along the crystallographic [100] direction is disordered over two general positions with a site occupancy of 81.8%. The eight-coordinated polyhedra include two binding modes of c1, two c2, two d1, and one d2 carboxylate oxygen donors (Figure 2). The observed Sr−O bond distances of binding modes of type c1 and d2 are longer than c2 and d1 (Table 4). Compared with compounds **1** and **2**, as expected, as the cation size and

dx.doi.org/10.1021/cg301471r | Cryst. Growth Des. 2013, 13, 326−332

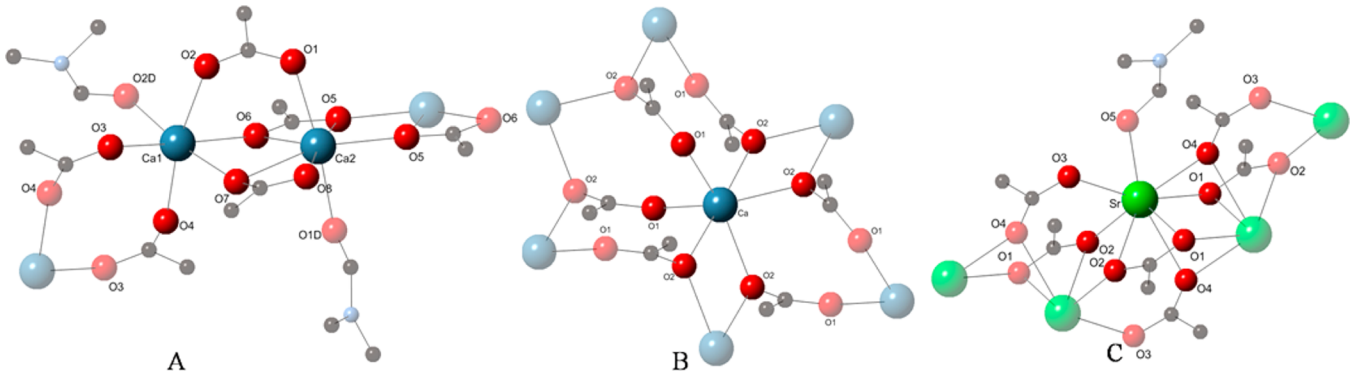

Figure 2. Different binding modes of $-COO^-$ groups of TDC ligand in compounds **1** (A), **2** (B), and **3** (C). Red spheres represent oxygen; black, carbon; and blue, nitrogen.

Table 2. Selected Bond Lengths (Å) and Angles (°) for Structure 1[a]

Ca(1)−[a]O(2)	2.316(3)	O(4)#3−Ca(1)−O(3)#2	88.9(1)
Ca(1)−O(2D)	2.320(3)	O(4)#3−Ca(1)−O(2)#1	169.2(1)
Ca(1)−[a]O(3)#1	2.302(2)	O(4)#3−Ca(1)−O(2D)	93.9(1)
Ca(1)−[a]O(4)#2	2.256(3)	O(4)#3−Ca(1)−O(7)#4	92.11(9)
Ca(1)−[c1]O(6)	2.431(2)	O(4)#3−Ca(1)−O(6)	85.43(8)
Ca(1)−[b3]O(7)#3	2.343(2)	O(3)#2−Ca(1)−O(2)#1	89.02(9)
Ca(2)−[a]O(1)	2.293(3)	O(3)#2−Ca(1)−O(2D)	90.1(1)
Ca(2)−O(1D)	2.290(3)	O(3)#2−Ca(1)−O(7)#4	92.78(9)
Ca(2)−[b2]O(5)#4	2.293(2)	O(3)#2−Ca(1)−O(6)	172.39(8)
Ca(2)−[c2]O(5)	2.441(2)	O(2)#1−Ca(1)−O(2D)	92.1(1)
Ca(2)−[c2]O(6)	2.504(2)	O(2)#1−Ca(1)−O(7)#4	81.33(9)
Ca(2)−[b2]O(7)	2.484(2)	O(2)#1−Ca(1)−O(6)	85.16(8)
Ca(2)−[b1]O(8)	2.360(3)		

[a]Symmetry codes: (#1) 0.5 − *x*, 0.5 + *y*, 1.5 − *z*; (#2) 0.5 + *x*, 0.5 − *y*, −0.5 + *z*; (#3) 0.5 + *x*, 0.5 − *y*, 0.5 + *z*; (#4) 1 − *x*, −*y*, 1 − *z*. For superscript letters a−c, see Scheme 1.

Table 3. Selected Bond Lengths (Å) and Angles (°) for Structure 2[a]

Ca−[d2]O(1)	2.300(2)	O(1)−Ca−O(2)#2	93.66(5)
Ca−O(1)#1	2.300(2)	O(1)−Ca−O(2)#3	157.08(5)
Ca−[d1]O(2)#2	2.393(1)	O(1)−Ca−O(2)#4	84.70(6)
Ca−O(2)#3	2.393(1)	O(1)−Ca−O(2)#5	93.80(6)
Ca−O(2)#4	2.394(1)	O(2)#2−Ca−O(2)#3	87.24(5)
Ca−O(2)#5	2.394(1)	O(2)#2−Ca−O(2)#4	108.34(5)
O(1)−Ca−O(1)#1	94.269(6)	O(2)#2−Ca−O(2)#5	73.33(5)

[a]Symmetry codes: (#1) *x*, 0.5 − *y*, −*z*; (#2) −1 + *x*, *y*, *z*; (#3) −1 + *x*, 0.5 − *y*, −*z*; (#4) 1 − *x*, 0.5 + *y*, *z*; (#5) 1 − *x*, −*y*, −*z*. For superscript letters d1−d2, see Scheme 1.

coordination number increase, the tendency for metal−oxygen distances increases. Overall, four equivalent oxygen atoms (two O1, two O4) form the shared rectangular face of the polyhedron while two equivalent oxygens (O2) generate the shared edge. The O3 and O5 atoms complete the eight-coordinate polyhedra. The connectivity in compound **3** differs from that of **1** and **2**. Edge- and face-sharing strontium polyhedra form chains, which are interconnected by TDC-2H linkers, resulting in the formation of a three-dimensional array (Figure 4).

3.4. Results and Discussion. For calcium-thiophenedicarboxylates, three different solvent systems—DMF, ethanol, and water—as well as their 1:1 volumetric combination were applied at two different synthesis temperatures in our preliminary study (Supporting Information Table S1). The reaction in pure DMF at 100 °C resulted in the formation of compound **1**, and reaction in pure ethanol at 100 °C leads to the formation of compound **2**. Other reactions (Supporting Information Table S1) at temperatures of both 100 and 180 °C have produced either a clear solution or unidentified microcrystalline compounds. The two synthetic routes were further explored to synthesize strontium-based TDC networks. The

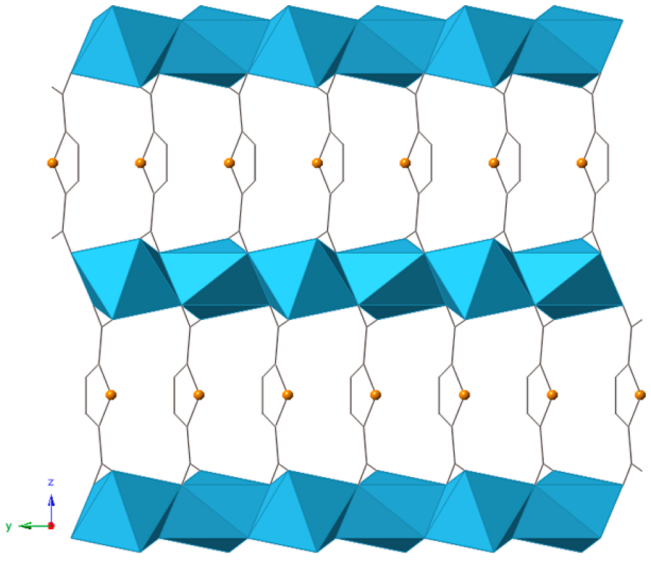

Figure 3. View of compound **2** along [100] showing chains of edge-linked calcium-centered, octahedra (blue), connected by the TDC-2H ligand. Sulfur is represented by spheres, and carbon, as wire bonds. Hydrogen atoms were omitted for clarity.

Table 4. Selected Bond Lengths (Å) and Angles (°) for Structure 3[a]

Sr−[c2]O(1)	2.734(1)	O(1)−Sr−O(1)#1	98.73(3)
Sr−[c1]O(1)#1	2.592(1)	O(1)−Sr−O(2)#2	123.62(3)
Sr−[c1]O(2)#2	2.433(1)	O(1)−Sr−O(2)	80.88(3)
Sr−[c2]O(2)	2.722(1)	O(1)−Sr−O(3)#3	95.99(4)
Sr−[d2]O(3)#3	2.494(1)	O(2)−Sr−O(3)#3	70.21(3)
Sr−[d1]O(4)#4	2.577(1)	O(2)#−Sr−O(4)#4	166.69(3)
Sr−[d1]O(4)	2.697(1)	O(3)#3−Sr−O(4)#4	106.89(4)
Sr−O(5)	2.530(1)	O(5)−Sr−O(1)#1	77.06(4)

[a]Symmetry codes: (#1) 1 − *x*, −*y*, −*z*; (#2) −*x*, −*y*, −*z*; (#3) 0.5 + *x*, 0.5 − *y*, 0.5 + *z*; (#4) 0.5 − *x*, −0.5 + *y*, −0.5 − *z*. For superscript letter c−d, see Scheme 1.

dx.doi.org/10.1021/cg301471r | *Cryst. Growth Des.* 2013, 13, 326−332

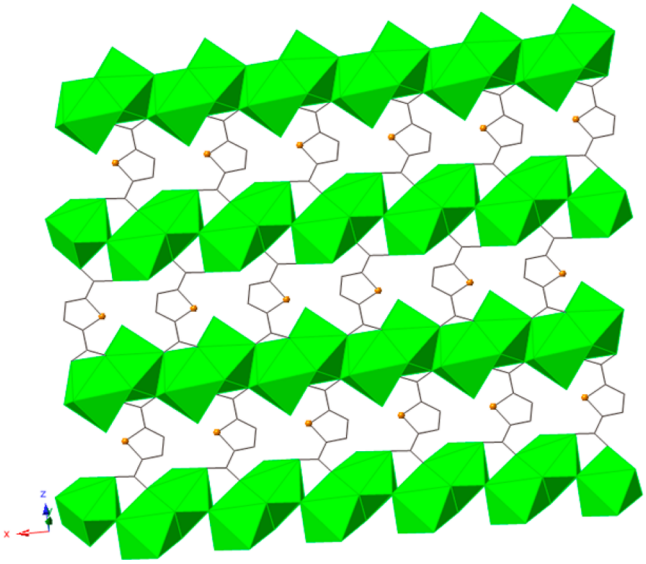

Figure 4. The connectivity of the TDC-2H with metal polyhedra in compound **3**. Strontium atoms are represented as green polyhedra, sulfur as spheres, and carbon as wire bonds. DMF solvent and hydrogen atoms were omitted for clarity.

use of DMF as a synthetic solvent at 100 °C resulted in the formation of compounds **3**. The use of ethanol as solvent at 100 °C resulted in the formation of a crystalline material (referred to as compound **4** [a = 5.7414(3) Å, b = 6.6227(3) Å, c = 9.8886(5) Å, α = 109.553(3)°, β = 106.896(3)°, γ = 89.983(3)°]), but a good structural model could not be achieved due to complex twinning of the crystals. However, the preliminary structure model, powder XRD pattern, thermogravimetric analysis, and photoluminescence measurements indicate that compound **4** is based on the strontium metal and TDC linker without incorporated solvent, similar to **2** (Figures 5 and 6, Supporting Information S11, S15).

The formation of compounds **1**−**4** is obtained by changing the synthetic solvent while the conditions remain the same (solvothermal, 100 °C). DMF coordinates with the metal centers, and the presence of water/ethanol leads to the formation of dense networks. This is contrary to our observations in the case of our earlier reported magnesium−

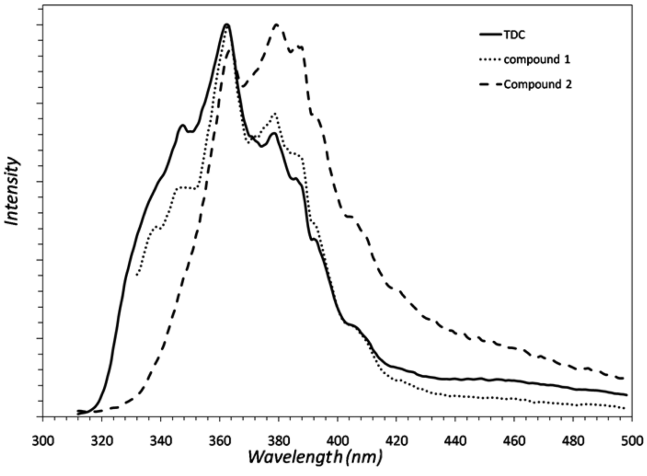

Figure 5. Comparison of luminescence spectra of **1** and **2** with TDC free linker.

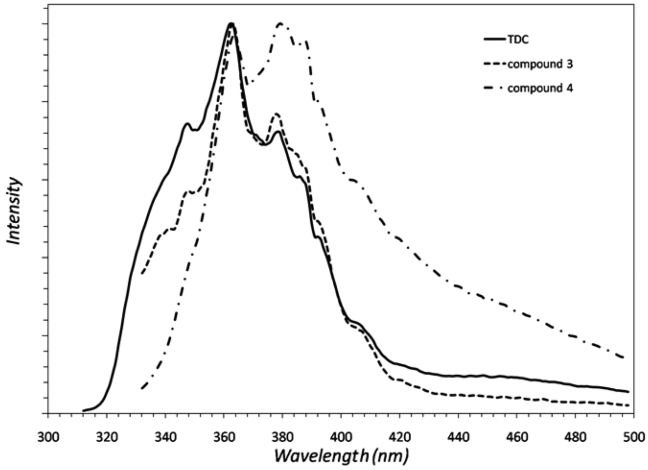

Figure 6. Comparison of luminescence spectra of **3** and **4** with TDC free linker.

pyridinedicarboxylate system,[37] in which the presence of water dictates the structural topologies. In the current case, the size of the solvent molecules, the coordination environment of the metal centers, and the coordination modes of the carboxylate groups play the key role. Carboxylate group binding modes influence the metal−oxygen bond distances, which increase from mode a through modes d2/b3 and b1 to d1/b2/c1 and c2, corresponding to from the monodentate to multidentate binding modes. (Table 5) In our previous study of Mg−TDC networks,[32] the binding of the carboxylate moieties contains one bridging coordination mode (mode a) and one bidentate mode, with the average bond lengths of Mg−O increasing from 2.063(1) to 2.193(1) Å, further proving that as the cation sizes increase, the carboxylate groups tend to bind larger numbers of metal ions when compared with our current work.

The thermal stabilities of the compounds **1**−**4** were investigated using a combination of simultaneous TGA−DSC techniques under N_2 atmosphere. TGA of compound **1** (Supporting Information Figure S12) shows two major weight losses during heating, with the first occurring at 340 °C, matching the removal of the two DMF solvent molecules (calculated, 25.8 wt %; observed, 25.2 wt %). The second major weight loss at 510 °C can be attributed to the pyrolysis of half of the TDC-2H linkers in the compound; 30.3 wt % loss calculated compared with 30.1 wt % observed. High thermal stabilities were observed for compounds **2** (Supporting Information Figure S13) up to ∼460 °C, with the first weight loss 39.1 wt % observed compared with the calculated 40.9 wt % expected from the decomposition of half of the TDC-2H linkers in the compound. Thermogravimetric analysis of compound **3** (Supporting Information Figure S14) also reveals two distinct weight losses during heating: an observed weight loss of 21.8 wt % at 300 °C compared with 21.2 wt % loss expected for removal of the coordinated DMF molecules. The second major weight loss of 27.2 wt % occurs at 500 °C and matches the 26.7 wt % loss corresponding to the pyrolysis of half of the TDC-2H linkers.

Photoluminescence studies were further conducted to gain insights into metal-linker interactions. The comparison of the luminescence spectrum of the synthesized compounds with that of the free linker enables us to examine how luminescence behavior changes with network topology. The calcium- and strontium-based TDC networks were examined in the same

dx.doi.org/10.1021/cg301471r | Cryst. Growth Des. 2013, 13, 326−332

Table 5. Bond Lengths (Å) of Different Binding Types of Carboxylate Groups in Compounds 1−3

		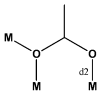					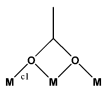	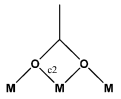
mode	a	d2	b3	b1	d1	b2	c1	c2
Ca								
min	2.256 (3)	2.300(2)	2.343(2)	2.360(3)	2.393(1)	2.484(2)	2.431(2)	2.441(2)
max	2.316(3)				2.394(1)	2.293(2)		2.504(2)
avg.	2.292(3)				2.3935(10)	2.388(2)		2.472(2)
Sr								
min		2.494(1)			2.577(1)		2.433(1)	2.722(1)
max					2.697(1)		2.592(1)	2.734(1)
avg.					2.637(1)		2.512(1)	2.728(1)

manner as in our previous studies to better understand the effect of network topologies on the photoluminescence properties. The free linker and compounds **1** and **3** show similar behavior when excited at 300 nm, with no significant difference in intensity noted between the ligand and the compounds. The broad peak centered at 363 nm in free linker is red-shifted to ∼379 nm in compounds **2** and **4**, while no significant peak shift is observed in case of compounds **1** and **3** (Figure 5 and 6). The structures of **1** and **3**, **2** and **4** are related, and the differences in the emission shifts are likely due to differences in the binding modes of the TDC carboxylates to the metal center and the terminal solvent (DMF). In our previous reports of novel magnesium TDC networks[32] which contains coordinated DMF and water molecules, we showed that the observed luminescence spectra for the networks were both red-shifted and of much higher intensity than that of the free linker, although in our current case, the red shift is only observed in compound **2**.

A similar effect was noted by Fang and co-workers in a zinc network linked by 1,3,5-benzenetricarboxylic acid, coordinated with DMF and water molecules, reporting only a red shift and not a significant difference in intensity of luminescence when comparing the free linker to the network compound.[38] Although the presence of a heteroatom in the aromatic ring could be the reason for the enhanced luminescence, a number of parameters, including crystal packing and the coordination environment of metal centers and linkers, also influence such a physical effect. In comparison with our previous work with Mg-TDC,[32] the red shifts observed in the current case suggests that crystal packing forces might control the ligand-to-metal charge transfer (LMCT) and thus also control the photoluminescence properties of the networks.

CONCLUSIONS

Four alkaline-earth metal-based coordination networks were synthesized under solvothermal conditions, with the variation of synthesis solvents leading to the formation of different topologies. Coordination environments of metal centers, binding modes of carboxylate groups of the linker, and the coordinated solvents influence the structures and properties. Comparing the three successfully solved structures and the photoluminescence measurements, it is noteworthy that the nature of the crystal packing is the major determinant of luminescence properties for *s*-block metal-based networks. Those networks coordinated with DMF molecules show no significant differences of photoluminescence intensity compared with the TDC linker, whereas networks with metals not coordinated with solvent molecules have photoluminescence peaks that are red-shifted. The detailed structural characterization of compounds **1**−**3** by single crystal XRD and thermal and photoluminescence measurements indicate that exploring *s*-block metal-based networks with luminescent organic ligands may helps us develop good candidates for lightweight photoactive materials.

ASSOCIATED CONTENT

Supporting Information

Summary of reaction conditions of Table 1 and Figures S1−S15, including the metal coordination sphere of compounds **1**−**3**, local environment of the metal ions in compounds **1**−**3**, PXRD data, and TGA data for the investigated compounds. X-ray crystallographic information files (CIF) are available for compounds **1**−**3**. CCDC 900825−900827 contain the supporting crystallographic data, which can be obtained free of charge from the Cambridge Crystallographic Data Centre via www.ccdc.cam.ac.uk/data_request/cif. This information is available free of charge via the Internet at http://pubs.acs.org/.

AUTHOR INFORMATION

Corresponding Author

*(J.B.P.) Phone: (631) 632 8196. Fax: (631) 632 8240 255. E-mail: john.parise@stonybrook.edu. (D.B.) Phone: (631)-632-1247. Fax: (631) 632 8240 255. E-mail: debasis.banerjee@stonybrook.edu.

Notes

The authors declare no competing financial interest.

ACKNOWLEDGMENTS

The work of the authors, including synthesis, characterization, analysis and preparation of the manuscript is supported by the U.S. Department of Energy, Office of Science, Office of Basic Energy Sciences, under contract DE-FG02-09ER46650. Crystal structures of **1**−**2** were determined using the Stony Brook University Single-Crystal Diffractometer, obtained through the support of the NSF (CHE-0840483). The structure of **3** was determined using data collected at ChemMatCars (Sector 15), Advanced Photon Source, principally supported by the NSF (CHE-0535644). Use of the Advanced Photon Source was supported by the U.S. Department of Energy, Office of Science, Office of Basic Energy Sciences, under Contract No. DE-AC02-

06CH11357. The authors acknowledge Zhichao Hu and Prof. Jing Li (Department of Chemistry, Rutgers University) for help during collection of the luminescence spectra.

REFERENCES

(1) Banerjee, D.; Parise, J. B. *Cryst. Growth Des.* **2011**, *11*, 4704.
(2) Tan, J. C.; Cheetham, A. K. *Chem. Soc. Rev.* **2011**, *40*, 1059.
(3) Sumida, K.; Rogow, D. L.; Mason, J. A.; McDonald, T. M.; Bloch, E. D.; Herm, Z. R.; Bae, T. H.; Long, J. R. *Chem. Rev.* **2012**, *112*, 724.
(4) Ma, S.; Zhou, H. C. *Chem. Commun. (Cambridge)* **2010**, *46*, 44.
(5) Murray, L. J.; Dinca, M.; Long, J. R. *Chem. Soc. Rev.* **2009**, *38*, 1294.
(6) Liu, J.; Thallapally, P. K.; McGrail, B. P.; Brown, D. R.; Liu, J. *Chem. Soc. Rev.* **2012**, *41*, 2308.
(7) Thallapally, P. K.; Grate, J. W.; Motkuri, R. K. *Chem. Commun.* **2012**, *48*, 347.
(8) Bordiga, S.; Regli, L.; Bonino, F.; Groppo, E.; Lamberti, C.; Xiao, B.; Wheatley, P. S.; Morris, R. E.; Zecchina, A. *Phys. Chem. Chem. Phys.* **2007**, *9*, 2676.
(9) Fernandez, C. A.; Liu, J.; Thallapally, P. K.; Strachan, D. M. *J. Am. Chem. Soc.* **2012**, *134*, 9046.
(10) Shah, M.; McCarthy, M. C.; Sachdeva, S.; Lee, A. K.; Jeong, H. K. *Ind. Eng. Chem. Res.* **2012**, *51*, 2179.
(11) Millange, F.; Guillou, N.; Medina, M. E.; Ferey, G.; Carlin-Sinclair, A.; Golden, K. M.; Walton, R. I. *Chem. Mater.* **2010**, *22*, 4237.
(12) Wu, P. Y.; Wang, J.; He, C.; Zhang, X. L.; Wang, Y. T.; Liu, T.; Duan, C. Y. *Adv. Funct. Mater.* **2012**, *22*, 1698.
(13) Bloch, E. D.; Murray, L. J.; Queen, W. L.; Chavan, S.; Maximoff, S. N.; Bigi, J. P.; Krishna, R.; Peterson, V. K.; Grandjean, F.; Long, G. J.; Smit, B.; Bordiga, S.; Brown, C. M.; Long, J. R. *J. Am. Chem. Soc.* **2011**, *133*, 14814.
(14) Forster, P. M.; Burbank, A. R.; Livage, C.; Ferey, G.; Cheetham, A. K. *Chem. Commun. (Cambridge)* **2004**, 368.
(15) Senkovska, I.; Kaskel, S. *Eur. J. Inorg. Chem.* **2006**, *2006*, 4564.
(16) Plonka, A. M.; Banerjee, D.; Parise, J. B. *Cryst. Growth Des.* **2012**, *12*, 2460.
(17) Gai, Y. L.; Jiang, F. L.; Xiong, K. C.; Chen, L.; Yuan, D. Q.; Zhang, L. J.; Zhou, K.; Hong, M. C. *Cryst. Growth Des.* **2012**, *12*, 2079.
(18) Paz, F. A. A.; Klinowski, J.; Vilela, S. M. F.; Tome, J. P. C.; Cavaleiro, J. A. S.; Rocha, J. *Chem. Soc. Rev.* **2012**, *41*, 1088.
(19) Saines, P. J.; Barton, P. T.; Jain, P.; Cheetham, A. K. *CrystEngComm* **2012**, *14*, 2711.
(20) Tremelling, G. W.; Foxman, B. M.; Landee, C. P.; Turnbull, M. M.; Willett, R. D. *Dalton Trans.* **2009**, 10518.
(21) Zhao, L. M.; Zhang, Z. J.; Zhang, S. Y.; Cui, P.; Shi, W.; Zhao, B.; Cheng, P.; Liao, D. Z.; Yan, S. P. *CrystEngComm* **2011**, *13*, 907.
(22) Fromm, K. M. *Coord. Chem. Rev.* **2008**, *252*, 856.
(23) Ferey, G. *Chem. Soc. Rev.* **2008**, *37*, 191.
(24) Williams, C. A.; Blake, A. J.; Wilson, C.; Hubberstey, P.; Schroeder, M. *Cryst. Growth Des.* **2008**, *8*, 911.
(25) Banerjee, D.; Kim, S. J.; Li, W.; Wu, H.; Li, J.; Borkowski, L. A.; Philips, B. L.; Parise, J. B. *Cryst. Growth Des.* **2010**, *10*, 2801.
(26) Chen, Z.; Zuo, Y.; Li, X.-H.; Wang, H.; Zhao, B.; Shi, W.; Cheng, P. *J. Mol. Struct.* **2008**, *888*, 360.
(27) Huang, W.; Wu, D. Y.; Zhou, P.; Yan, W. B.; Guo, D.; Duan, C. Y.; Meng, Q. J. *Cryst. Growth Des.* **2009**, *9*, 1361.
(28) Gong, Y.; Wang, T.; Zhang, M.; Hu, C. W. *J. Mol. Struct.* **2007**, *833*, 1.
(29) Chen, Z.; Zuo, Y.; Li, X. H.; Wang, H.; Zhao, B.; Shi, W.; Cheng, P. *J. Mol. Struct.* **2008**, *888*, 360.
(30) Wang, J. G.; Huang, C. C.; Huang, X. H.; Liu, D. S. *Cryst. Growth Des.* **2008**, *8*, 795.
(31) El Osta, R.; Frigoli, M.; Marrot, J.; Medina, M. E.; Walton, R. I.; Millange, F. *Cryst. Growth Des.* **2012**, *12*, 1531.
(32) Calderone, P. J.; Banerjee, D.; Santulli, A. C.; Wong, S. S.; Parise, J. B. *Inorg. Chim. Acta* **2011**, *378*, 109.
(33) Allendorf, M. D.; Bauer, C. A.; Bhakta, R. K.; Houk, R. J. *Chem. Soc. Rev.* **2009**, *38*, 1330.
(34) Cui, Y.; Yue, Y.; Qian, G.; Chen, B. *Chem. Rev.* **2012**, *112*, 1126.
(35) *CrysAlis PRO. Verion 4*.Oxford Diffraction Ltd.: Yarnton, Oxfordshire, England, 2010.
(36) Sheldrick, G. M. *Acta Crystallogr., A* **2008**, *64*, 112.
(37) Banerjee, D.; Finkelstein, J.; Smirnov, A.; Forster, P. M.; Borkowski, L. A.; Teat, S. J.; Parise, J. B. *Cryst. Growth Des.* **2011**, *11*, 2572.
(38) Fang, Q. R.; Zhu, G. S.; Xue, M.; Sun, J. Y.; Sun, F. X.; Qiu, S. L. *Inorg. Chem.* **2006**, *45*, 3582.